Progress in Nuclear Energy 108 (2018) 358–371

Contents lists available at ScienceDirect

Progress in Nuclear Energy

journal homepage: www.elsevier.com/locate/pnucene

New turbulence modeling for simulation of Direct Contact Condensation in two-phase pressurized thermal shock

M. Ghafari[a,*], M.B. Ghofrani[a], F. D'Auria[b]

[a] Department of Energy Engineering, Sharif University of Technology, Azadi Ave., Tehran, Iran
[b] San Piero a Grado Nuclear Research Group (GRNSPG), University of Pisa, Via Livornese 1291, San Piero a Grado, Pisa, Italy

ARTICLE INFO

Keywords:
Pressurized water reactor
Pressurized thermal shock
Steam/water stratified flow
Condensation rate
Turbulence model

ABSTRACT

Injection of Emergency Core Cooling System (ECCS) water into the primary loops of the Pressurized Water Reactors (PWRs) leads to rapid cooling of Reactor Pressure Vessel (RPV) inside wall after Loss Of Coolant Accident (LOCA). This condition, known as Pressurized Thermal Shock (PTS) intensifies the propagation of the RPV structural defects and would be considered as an ageing mechanism. For structural and fracture analysis of RPV wall, thermal-hydraulic analysis of PTS should be accomplished to obtain the steam/water flow characteristics in the downcomer. For this purpose, simulation of steam/water stratified flow (due to density difference) after the injection point should be done by Computational Fluid Dynamics (CFD) methods. In this region, steam condensation over water layer is considered as the only heat source and controlled by turbulence eddy motion near the steam/water interface. Based on Surface Renewal Theory (SRT), Heat Transfer Coefficient (HTC) would be calculated by evaluation of turbulence length and velocity. Therefore, prediction of turbulence characteristics plays a significant role for estimation of interfacial mass transfer and temperature profile. High gradient of velocity and Turbulence Kinetic Energy (TKE), and interfacial mass and momentum transfer at the steam/water interface needs some modifications for application of traditional turbulence models. Implementation of damping function is one of the common solutions to overcome the overestimation of TKE at the steam/water interface. Although, this function improves flow characteristics of smooth stratified flow, investigation of conservation equations and experimental data implies that the other source function is needed when the flow regime changes to wavy flow. In this paper, a new source function of TKE based on variations of turbulence characteristics is proposed for steam/water interface leading to a special boundary condition of turbulence. To investigate the effects of this modification, simulation of air/water and steam/water stratified flow in three different test facilities is performed. The results show that the implementation of the source function of TKE improves the prediction of turbulence characteristics at the interface of isothermal stratified flow. Also condensation rate and temperature gradient of steam/water stratified flow have a better agreement with experimental data.

1. Introduction

Steam/water stratified flow would take place in normal or emergency conditions of industrial processes such as chemical process and nuclear power plant. In the primary loops of Pressurized Water Reactor (PWR), The Emergency Core Cooling System (ECCS) water enters the hot steam flow environment in the cold leg (while its temperature is between 283 K and 298 K) after some scenarios of Loss Of Coolant Accident (LOCA) (Lucas et al., 2007). As the new mixture of water and steam goes away from injection point into the Reactor Pressure Vessel (RPV), two-phase stratified flow propagates in the cold leg by means of density difference between water and steam. In this condition, the temperature reduction of the coolant leads to RPV overcooling and thermal load on it, known as Pressurized Thermal Shock (PTS). The prediction of plant response to LOCA by system codes and, temperature gradient in the RPV wall by CFD codes should be done in thermal-Hydraulic step of PTS analysis (Bestion, 2010; IAEA, 2003). For the second purpose, the simulation of stratification zone (after the injection point) plays a significant role for evaluation of water temperature and needs a special attention due to complex phenomena at the interface of steam and water (Griffiths et al., 2014).

In horizontal two-phase stratified flow; gravity, relative velocity, interfacial shear stress and surface tension of two phases dictate different flow pattern and interface shape (Lin and Hanratty, 1986). The

* Corresponding author.
E-mail address: ghaffari@energy.sharif.ir (M. Ghafari).

https://doi.org/10.1016/j.pnucene.2018.06.007
Received 12 September 2017; Received in revised form 11 May 2018; Accepted 11 June 2018
Available online 26 June 2018
0149-1970/

Nomenclature

A	Interfacial area density
a	Thermal diffusivity
C_μ	Proportional constant of eddy viscosity
g	Gravity acceleration
h	Bulk average enthalpy
K	Turbulence kinetic energy
P	Pressure
S	Source function
t	time
T	Temperature
U	Velocity
u,v,w	Horizontal, vertical and axial component of velocity
α	Volume fraction
B	Closure coefficient of the destruction term of k-ω model
γ	Closure coefficient of k-ω model (5/9)
σ_ω	Closure coefficient of k-ω model (0.5)
σ_k	Closure coefficient of k-ω model (0.5)
Γ	Interfacial mass transfer
ν	Kinematic viscosity
P	Density
λ	Thermal conductivity
τ	Shear stress
ω	Turbulence eddy frequency
ε	Turbulence eddy dissipation

Subscript and superscript

G	Gas phase
i	Interface
L	Liquid phase
T	Turbulence
Sat	Saturation
w	Water
S	Steam

high gradient of flow characteristics (e.g. velocity and turbulence kinetic energy) at the interface needs a special treatment to capture these variations. In addition to this fact, condensation of steam plume over the water layer would occur due to temperature gradient. Steam condensation and mass transfer between two phases lead to variation of temperature and flow rate without any heat source or sink which is known as Direct Contact Condensation (DCC). DCC includes 3D effects and local phenomena at the interface and needs a finer space resolution, especially at the interface (Bestion, 2010; Bian et al., 2017). Therefore, modeling of two-phase stratified flow containing interfacial mass and heat transfer is known as an ongoing research interest of Computational Fluid Dynamics (CFD). The key parameter controls the rate of condensation is Heat Transfer Coefficient (HTC) which strongly depends on length and velocity scale of turbulent eddies transferring thermal energy from interface into the fluid bulks.

The complexity of interfacial phenomena in two phase stratified flow led to development of related test facility for evaluation of different variables. Some of these facilities have been selected as validation test case for benchmarking procedure of new simulation codes. Fabre et al. (1987) used a rectangular channel for investigation of smooth and wavy air/water stratified flow. They measured velocity and turbulence characteristics by Helium-Neon laser and forward scattering method, respectively. Lim et al. (1984) investigated axial reduction of steam mass flow rate due to DCC in smooth and wavy stratified flow. They employed pitot tubes and conductivity probes for evaluation of steam velocity and water depth. Goldbrunner et al. (2002) considered water temperature gradient in steam/water smooth stratified flow and reported vertical temperature gradient and total condensation rate by implementation of linear Raman spectroscopy. Vallée et al. (2008), from HZDR institute, developed two rectangular test facilities for observation of interface shape and propagation of slug flow pattern. High-speed video and Particle Image Velocimetry (PIV) method were applied for these purposes. Lips and Meyer (2012) considered interfacial condensation in a small inclined pipe and studied the variation of HTC in different flow pattern. They also examined the maturity of different flow pattern maps based on experimental data. Ayati et al. (2014) investigated the velocity profile near the wall and interface of air/water stratified flow in a pipe of 31 m in length. They applied PIV measuring method with tracing of water droplets and considered both smooth and wavy stratified flow. Roman et al. (2016) developed an experimental facility based on neural network detection algorithm for identification of flow regime. They employed electrical capacitance tomography to distinguish between gas and liquid phase.

To find a practical approach for estimation of HTC, Higbie (1935) developed Surface Renewal Theory (SRT) calculating mass transfer rate as a function of surface renewal period. This period refers to the contact time of an eddy with gas and liquid. Danckwerts (1951) modified the Higbie (1935) theory by consideration of surface renewal rate and calculated mass transfer coefficient as a function of physical characteristics and renewal rate. Hughes and Duffey (1991) determined the renewal period by using of the Kolmogorov length and velocity scales and dissipation of energy in the liquid. Based on Kolmogorov theory, the energy of large eddies is transferred to small eddies and then, converted to thermal energy by viscosity at low Reynolds number (Kolmogorov, 1941). Akira et al. (1992) calculated HTC based on SRT and consideration of non-zero turbulence boundary condition at the interface. Shen et al. (2000) defined a boundary layer at the interface according to Gaussian reduction of turbulent eddy viscosity and proposed new turbulence length and velocity scale. Yao et al. (2005) considered the turbulence production of interfacial friction and compared the condensation of Lim et al. (1984) experiment by Shen et al. (2000) and Hughes and Duffey (1991) model. They reported underestimation of Shen et al. (2000) model and overestimation of Hughes and Duffey (1991) model for interfacial heat transfer. Also Ceuca and Macián-Juan (2012) compared the difference between these models for LAOKOON experiment and reported better results for Shen et al. (2000). Gada et al. (2016) investigated application of Hughes and Duffey (1991) model with Large Scale Interface (LSI) model for steam condensation in a pipe when cold water injected in it. They predicted total rate of condensation with some distortions for condensation in the pipe. Coste et al. (2008b) investigated the application of NEPTUNE CFD using large Interface Method (LIM) for simulation of interfacial mass and momentum transfer. They introduced a new HTC correlation based on SRT with some modifications for calculation of velocity and length scale. Štrubelj et al. (2010) used this correlation to predict the condensation in water hammer experiments and showed poor agreement between experimental and simulation results. In addition to SRT, Banerjee (1990) introduced Surface Divergence (SD) as a function of tangential fluctuation velocity gradient and used it instead of surface renewal period for eddy transport calculation. He calculated transfer velocity for unsheared interface based on Hunt and Graham (1978) blocking theory. Banerjee et al. (2004) employed SD model for sheared interface and showed that the relation of unsheared interface is valid with change of constant value. Also, Lakehal (2010) developed a new modeling strategy for simulation of DCC solving super grid turbulence and interfacial scales directly, whereas the sub-grid parts are modeled based on Interface Tracking Method (ITM) and Large Eddy Simulation (LES) turbulence model. Lakehal and Labois (2011) employed this new modeling strategy in SD model to calculate HTC and condensation rate in stratified flow. Li et al. (2015) employed LES turbulence model and

VOF method for simulation DCC of a steam injection into the water pool and showed the effects of steam velocity on condensation rate. Kadi et al. (2015) used this new strategy in TransAT code and considered a turbulence damping function at the interface like solid boundary condition. Ren et al. (2016) used mass fraction method for estimation of condensation in ECCS out nuzzle after LOCA and showed the conservative results for condensation rate.

The review of implemented approaches for HTC calculation reveals the importance of the turbulence characteristics prediction at steam/water interface. The high gradient of velocity and Turbulence Kinetic Energy (TKE) in this region needs a special treatment for exact prediction of turbulence characteristics (Bestion, 2010). The gradient of velocity generates high turbulence when differential eddy viscosity models like k-ε or k-ω are used (Egorov et al., 2004; Reboux et al., 2006). The employment of turbulence damping function decreasing turbulence and dictating a new boundary condition similar to solid boundary is a common solution to decrease turbulence (Wilcox, 1998). Although this modification improves the flow characteristics of smooth interface (Höhne and Mehlhoop, 2014), a considerable underestimation of TKE occurs when the flow pattern changes to transient or wavy flow. From the point of view of PTS thermal-hydraulic analysis, this shortcoming of traditional eddy viscosity models leads to inaccurate evaluation of condensation and coolant temperature in the cold leg after LOCA. Therefore, the other boundary condition should be implemented at the interface to bridge this gap. The investigation of transport equation of turbulence characteristics shows some differences between wall boundary condition and steam/water interface, especially for TKE which is considered equal to zero near a wall. The evaluation of turbulent characteristics profile resulted in proposing a new source function for TKE near the free surface. This function should be added to transport equation of TKE to improve underestimation of TKE at the interface. In addition of TKE, the proposed function changes the HTC, temperature profile and steam flow rate.

Section 2 of the current paper gives a review of conservation equation of mass, momentum, energy and turbulence characteristics, and different model and improvement employed in literature. Section 3 illustrates the procedure of new source function definition based on turbulence transport equation and in section 4 the new approach is employed for three different experiments including isothermal air/water and steam/water stratified flow.

2. Two phase stratified modeling

2.1. Flow regime identification in horizontal pipeline

The identification of the flow regime in horizontal pipes plays an important role for simulation of these flows. Models for the transition from stratified flow to slug flow (or intermediate flow) are based on Kelvin-Helmholtz instability theory. According to this theory, small waves will grow when (Lamb, 1932; Milne-Thompson, 1968):

$$(U_G - U_L) \geq \sqrt{\frac{(\rho_L - \rho_G) g h_G}{\rho_G}} \tag{1}$$

Where h_G is the gas phase height.

In addition to this criterion, there are the other instability conditions of stratified flow in literature considering more forces and phenomena at the interface. Thorpe (1969) studied dynamics aspect of instability in a rotated rectangular channel including two immiscible fluids experimentally and theoretically. Their results obtained the dynamics parameters such as critical wave-number and velocity disturbance and revealed the occurrence of Kelvin-Helmholtz and Tollmien-Schlichting instability. Lin and Hanratty (1986) developed linear Kelvin-Helmholtz stability theory to predict the onset of slug flow for air-water flow. They considered the inertia of liquid phase and shear stress neglected in inviscid theory and showed ignorance of these effects is valid only for very large liquid viscosities. Brocchini and Peregrine (2001) introduced L-q diagram for the interface shape identification based on magnitude of Froude number and Weber number for each point. They used turbulence kinetic energy and dissipation rate for calculation of turbulence length scale and velocity to predict the shape of the interface.

2.2. Conservation equations

For evaluation of condensation rate and temperature profile in steam/water stratified flow, modeling of non-resolved scales should be accomplished by utilization of statistic approaches. If appropriate models are employed for modeling of this motion, conservation equation of mass, momentum and energy would be effective to capture these phenomena (Bestion, 2010; Egorov et al., 2004). Two-fluid model, considering steam and water as two segregated streams (Collier and Thome, 1994), consists of six conservation equations (mass, momentum and energy for each phase) as follows (Ishii and Hibiki, 2010):

$$\begin{aligned}
&\frac{\partial \alpha_k \rho_k}{\partial t} + \nabla.(\alpha_k \rho_k U_k) = \Gamma_k \\
&\frac{\partial \alpha_k \rho_k U_k}{\partial t} + \nabla.(\alpha_k \rho_k U_k U_k) = -\alpha_k \nabla P + M_k + \alpha_k \rho_k g + \nabla.[\alpha_k(\tau_k + \tau_k^T)] \\
&\frac{\partial}{\partial t}\left[\alpha_k \rho_k \left(h_k + \frac{U_k^2}{2}\right)\right] + \nabla.\left[\alpha_k \rho_k \left(h_k + \frac{U_k^2}{2}\right) U_k\right] = \alpha_k \frac{\partial P}{\partial t} + \alpha_k \rho_k g.\, U_k + \Gamma_k\left(k_{ki} + \frac{U_k^2}{2}\right) \\
&+ A_i q''_{k,i} + q'''_{k,w} - \nabla.[\alpha_k(q_k + q_k^T)] \\
&k = L, G
\end{aligned} \tag{2}$$

In Eq. (2), M_k reveals the effect of interphase momentum transfer including Drag, lift, added mass, turbulence dispersion force and momentum associated to the interfacial transfer of mass. $A_i q''_{k,i}$ and $q'''_{k,w}$ are the heat exchange terms at the interface and wall per unit volume. Also q_k and q_k^T refer to the molecular and turbulence heat flux. The interfacial mass transfer per volume, Γ, is calculated by definition of interfacial HTC and consideration of temperature difference between steam and water (Štrubelj et al., 2010) as follows:

$$\Gamma = \frac{|\nabla\alpha| HTC\,(T_{sat} - T_w)}{h_{s,sat} - h_w} \tag{3}$$

where $|\nabla\alpha_i|$ refers to interfacial area density. As explained in the previous section, evaluation of eddy contact time (Higbie, 1935) and turbulent diffusivity (Danckwerts, 1951) are two main parameters related to HTC at the interface. For the first approach, calculation of surface renewal period is performed by introduction of length and velocity scale. These characteristics would be defined according to different phenomena and characteristics (e.g. shear velocity, turbulence intensity, film thickness, channel diameter). Since eddy contact time is proposed to provide an estimation of eddy motion, the use of turbulence characteristics at the steam/water interface would result in improvement of HTC evaluation. Among the recommended approaches for calculating of this quantity, Hughes and Duffey (1991) model based on Kolmogorov theory and Shen et al. (2000) model according to evaluation of eddy viscosity in sublayer has been considered as two major perspectives in previous studies. In the first theory, it is assumed that the total energy of the large eddies is transferred to the small eddies which can be considered statistically isotropic (Kolmogorov, 1941). Base on this theory and calculation of eddy contact time, the following equation is proposed for HTC at the interface:

$$HTC_1 = \frac{2}{\sqrt{\pi}} \rho C_P \sqrt{a} \left(\frac{\varepsilon}{\nu}\right)^{0.25} \tag{4}$$

In the second approach (estimation of eddy viscosity), a Gaussian function of eddy viscosity is proposed in a sublayer near the interface where the reduction of fluctuation velocity component occurs due to interface boundary condition. With this assumption, the other equation for calculation of HTC was proposed by Shen et al. (2000):

$$HTC_2 = 0.794\rho C_P \sqrt{a}\left(\frac{\varepsilon}{k}\right)^{0.5} \quad (5)$$

Regardless of the constant coefficient of Eq. (4) and (5) that have a slight effect on two models, the definition of turbulence length and velocity is considered as the fundamental difference between HTC_1 and HTC_2. Based on previous investigations, a considerable underestimation or overestimation of interfacial mass transfer would take place for different flow pattern in horizontal channel (Ceuca and Macián-Juan, 2012; Yao et al., 2005). Despite this difference, both relationships are significantly dependent on the correct estimation of turbulence characteristics at the steam/water interface. Therefore, some shortcomings of the mentioned equations would be related to turbulence modeling in this region. Therefore, the other researches in literature focused on improvement of turbulence modeling. With this division, the present paper can be categorized in the second group, which tries to predict DCC by improving the boundary conditions of turbulence characteristics. In the next section, some common methods used to improve the prediction of turbulence characteristic will be illustrated.

2.3. Turbulence modeling

The dependency of HTC on turbulence characteristics at the interface needs a special treatment. The high gradient of velocity near the interface is similar to flow condition near a wall. This condition dictates a specific behavior of turbulent characteristics that are not predicted by traditional two equations turbulence models. So, the other modifications should be considered to bridge the gap. Liovic and Lakehal (2007) employed large eddy simulation turbulence model at the interface of air jet injected into a water pool and demonstrated the effect of surface roughness on turbulence dissipation rate. Nourgaliev et al. (2008) introduced sharp interface method based on level set method to capture sharp variation of hydrodynamic characteristic by using a special function at the interface. Ayati et al. (2016) experimentally showed the effect of flow rate in stratified flow of air and water on generation of turbulence structure and dissipation of energy at the interface. Egorov et al. (2004) proposed that a turbulence damping function is employed near the free surface of the stratified flow according to wall function of k-ω model (Wilcox, 1998) using Taylor approximation for fluctuation velocity components as follows:

$$\begin{aligned} u' &= A(x,z)\Delta y + B(x,z)\Delta y^2 + \ldots \\ v' &= A'(x,z)\Delta y + B'(x,z)\Delta y^2 + \ldots \\ w' &= A''(x,z)\Delta y + B''(x,z)\Delta y^2 + \ldots \end{aligned} \quad (6)$$

The fluctuating velocity satisfies no-slip boundary condition and conservation of mass (Wilcox, 1998). As a result, the following equation should be equal to zero when Δy tends to zero:

$$\frac{\partial u'}{\partial x} + \frac{\partial v'}{\partial y} + \frac{\partial w'}{\partial z} = A'(x,z) + O(\Delta y) \quad (7)$$

Consideration of Eq. (7) implies that $A'(x,z)$, due to lack of dependency on y, should be zero. Consequently, the fluctuating velocity components behave as follows:

$$\begin{aligned} u' &= A(x,z)\Delta y + O(\Delta y^2), \\ v' &= A'(x,z)\Delta y^2 + O(\Delta y^3), \\ w' &= A''(x,z)\Delta y + O(\Delta y^2). \end{aligned} \quad (8)$$

Substitution of velocity component in the definition of K and ω obtains the variation of these variables near a wall as follows:

$$k \sim \Delta y^2 \quad (9)$$

$$\omega \sim \frac{\nu}{\beta \Delta y^2} \quad (10)$$

The same result can would be obtained by consideration of standard transport equations of k and ω which is more favorable for interface of gas and liquid. The standard transport equations of k-ω model are (Wilcox, 1998):

$$\partial_t k + u.\nabla k = P_k - C_\mu \omega k + \nabla.[(\nu + \sigma_k \nu_t)\nabla k] \quad (11)$$

$$\partial_t \omega + u.\nabla \omega = \frac{\gamma\omega}{k} P_k - \beta\omega^2 + \nabla.[(\nu + \sigma_\omega \nu_t)\nabla \omega] \quad (12)$$

where P_k is turbulence production term.

By consideration of velocity components near a solid boundary, these transport equations would be reduced in steady state condition and non-dimensional form as follow (Kalitzin et al., 2005):

$$\frac{\partial^2 \omega^+}{\partial y^{+2}} - \beta\omega^{+2} = 0 \quad (13)$$

$$\frac{\partial^2 k^+}{\partial y^{+2}} - c_\mu k^+ \omega^+ = 0 \quad (14)$$

Where

$$k^+ = \frac{k}{u_\tau^2},\ \nu^+ = \frac{\nu}{u_\tau},\ y^+ = \frac{y u_\tau}{\nu},\ \omega^+ = \frac{\omega\nu}{u_\tau^2}$$

The singular solution of (13) satisfying the flow conditions at the solid boundary is the same that previous function of Turbulence Eddy Frequency (TEF) (Eq. (10)). The following value of TEF is employment for definition of a source function which is known as turbulence damping function:

$$\omega^+ = \frac{6B}{\beta y^{+2}} \quad (15)$$

where B is a coefficient, which should be selected big enough, at least 10 (bigger values do not change the result for a solid wall) (Egorov et al., 2004; Höhne and Mehlhoop, 2014). Using the value for TEF implies that the behavior of TKE is according to Eq. (9). Therefore, the gradient of TKE and its gradient will be zero which does not conform with TKE profile near the free surface of a two-phase stratified flow. Höhne and Mehlhoop (2014) used this damping function in AIAD (Algebraic Interfacial Area Density) method for case 250 and case 400 of Fabre et al. (1987) experiment. The rationale behind AIAD model is the selection of the drag coefficient based on local morphology detection (Höhne and Lucas, 2011). Drag coefficient of gas bubbles, liquid droplets and free surface at the interface is calculated separately and overall drag coefficient is a weighted sum of them. Although they improved the velocity profile of case 250, but deviations reveal in case 400 which the vertical motion of the free surface is considerable. The investigation of two-phase phenomena occurring in a wavy stratified flow shows that the utilization of damping function is not sufficient. In addition to velocity, TKE has a sharp variation which is considered equal to zero near the wall. Obviously, the behavior of interface differs from solid boundary condition in some features affecting the flow characteristics and the other modification is needed for TKE boundary condition illustrated in the next section.

3. New turbulence model near the free surface

Consideration of vertical component of velocity and nonzero boundary condition of TKE and its gradient at the interface are two important factors neglected in the previous turbulence models and this paper focused on a new model based on them. If the TEF value of Wilcox (1998) wall function is substituted in reduced transport equation of TKE (Eq. (14)), this equation can be solved as:

$$k^+(y^+) = C_1(y^+)^{\left(\frac{1-\sqrt{1+4\xi}}{2}\right)} + C_2(y^+)^{\left(\frac{1+\sqrt{1+4\xi}}{2}\right)} \quad (16)$$

Where:

$$\xi = \frac{6C_\mu}{\beta}$$

The powers of the first and second term in Eq. (16) are negative and positive. For wall boundary condition, it is assumed that the value of TKE and its gradient are equal to zero. So, the first term of Eq. (16) should be ignored and only positive power considered for wall function. If this boundary condition is applied for the interface of steam and water, no special treatment is needed for TKE. But, the investigation of experimental results shows that these boundary conditions of TKE, have no consistency with the variation of TKE (Apanasevich et al., 2015; Höhne and Mehlhoop, 2014; Yao et al., 2005). Therefore, the non-zero boundary conditions of TKE and its gradient are needed at the interface of steam and water. Based on this point, the first term of Eq. (16) should be taken into account to reveal the value of TKE and its gradient. On the other, the second term of Eq. (16) tends to zero when the distance of interface decreases. As the modification of TKE will be implemented at the interface (where y^+ is small), it is possible to ignore this term in Eq. (16). By this assumption, one boundary condition is needed to specify the constant C_1.

There is no explicit boundary condition at the interface due to lack information of TKE. As the TKE is a continues function in vertical direction, it is possible to assume that the value of TKE (according to Eq. (16)) approaches to value of turbulence kinetic energy far from the interface where no turbulence source function will be implemented. As a result of this assumption, a certain distance from interface and a value of TKE are considered for calculation of constant C_1 in Eq. (16). This distance should be far enough from the interface that interfacial effects could be ignored. The selection of this distance may have a major effect on the TKE profile. So, a sensitivity study is necessary to assess the impact of this boundary condition. For the first evaluation, the distance of $y^+ = 400$ is considered for this purpose. Also, the average value of TKE at the Log-law layer near the wall (where $30 < y^+ < 300$ (Versteeg and Malalasekera, 2007)) is considered as value of source function at the proposed distance from the interface. This boundary condition leads to decreasing function for TKE when the distance from the interface increases and the maximum value of TKE source function will occur at the interface. This behavior is similar to the first term of Eq. (16) tending to C_1 when y^+ increases. Consideration of the positive term in Eq. (16) will increase TKE source function which should be zero out of the interface. Also, the TKE and TEF source function will be implemented in steam/water interface where interfacial area density is a non-zero function, and the positive term for TKE source function has no effect on interfacial parameters. Therefore, the positive term is neglected and the value of TKE at the interface would be obtained as follows:

$$k^+(y^+) = \overline{k_{Log-layer}}\left(\frac{y^+}{400}\right)^{\left(\frac{1-\sqrt{1+4\xi}}{2}\right)} \tag{17}$$

In addition to boundary condition modification, consideration of vertical motion of interface affects the value of turbulence characteristics. This difference between solid boundary condition and steam/water interface intensifies when the interface changes from smooth to wavy shape. The vertical motion of small waves produced by Kelvin-Helmholtz instability would increase TKE at the interface. This phenomenon implies that the convection transport term of TKE and TEF in vertical direction would affect the source function value of them. For investigation of vertical velocity effects, the vertical convection terms of TKE and TEF are added to reduced transport equations (Eq. (13) and (14)) as follows:

$$\frac{\partial^2\omega^+}{\partial y^{+2}} - v^+\frac{\partial\omega^+}{\partial y^+} - \beta\omega^{+2} = 0 \tag{18}$$

$$\frac{\partial^2 k^+}{\partial y^{+2}} - v^+\frac{\partial k^+}{\partial y^+} - C_\mu\omega^+k^+ = 0 \tag{19}$$

Unlike the previous reduced transport equations, no analytical solution can be considered for Eq. (18) and (19). In addition to this fact, the vertical component of velocity would be a function of y^+ at the interface and should be evaluated for solving these equations. As a result, only the numerical solution can be employed to find TKE and TEF function. For numerical solution of Eq. (18) and (19) with the assumptions illustrated in the previous paragraph, two different boundary conditions are needed for both differential equations. The first type of boundary condition proposed in this section is similar to Eq. (17) and it is supposed that both ω^+ and k^+ are known far from the interface ($y^+ = 400$). The second boundary condition is defined due to reduction of turbulence source far from the interface. Actually, the source function of TKE and TEF will be employed near the free surface where the interfacial area density is large enough. In this region, the magnitude of both sources should be very large and decreases when the y^+ increases. This behavior is similar to Eq. (17) without any consideration of vertical velocity. So, it is supposed that the variation of turbulence sources far from the interface is equal to zero where those terms have no effect on transport equations. By consideration of these boundary conditions, numerical method can be implemented for solving of Eq. (18) and (19). Fig. 1 and Fig. 2 depict the profile of TKE and TEF by implementation of proposed boundary conditions and numerical solution for different value of V^+. As shown in these figures, the convection term of both equations has a considerable effect of turbulence magnitude at the free surface. For high positive value of vertical velocity, turbulence energy and dissipation rate decreases due to eddy transport out of interface while higher turbulence reveals when the vertical velocity is negative.

For implementation of this new turbulence model, the numerical solution of two transport equations should be accomplished for each point at the interface in all iteration leading to time-consuming calculation procedure. So, for the first evaluation, the effect of vertical velocity will be ignored and the value of TKE and TEF be calculated based

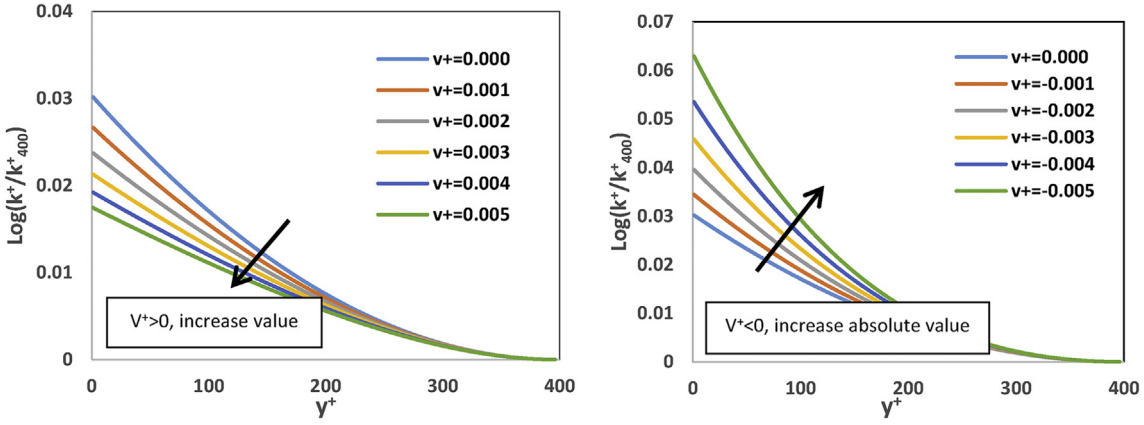

Fig. 1. Turbulence kinetic energy profile near the free surface for positive and negative value of V^+.

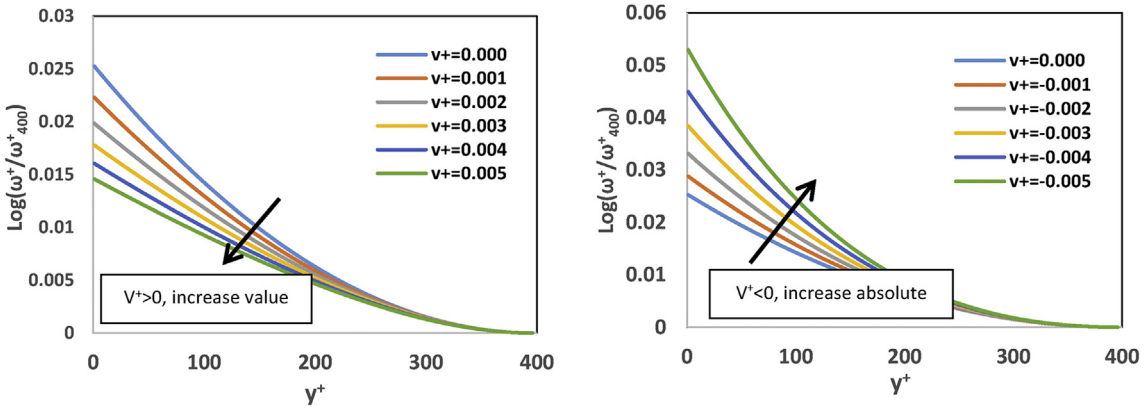

Fig. 2. Turbulence eddy frequency profile near the free surface for positive and negative value of V^+.

on Eq. (15) and (17). These values are added to transport equations as two following source functions:

$$S_k = \rho_i U_i |\nabla \alpha_i| k$$
$$S_\omega = \rho_i \Delta y \beta |\nabla \alpha_i| \omega^2$$
$$i = w, s \tag{20}$$

where $|\nabla \alpha_i|$ is the value of interfacial area density and guarantees the application of the source functions near the free surface.

4. Validation of new turbulence function

In this section some experiments about two-phase stratified flow are selected to evaluate the effect of turbulence modification at interface of two phases. In the first experiment, an adiabatic co-current air and water flow passes through a rectangular channel is considered as an isothermal stratified flow. The measurement of velocity and turbulence characteristics is performed at vertical line at a distance of 9.1 m from inlet (Fabre et al., 1987). The second experiment focuses on temperature profile in a smooth stratified flow of steam and water in a rectangular channel and condensation occurs at the interface (Goldbrunner et al., 2002). In the last experiment containing wavy flow of steam and water, the reduction of steam flow rate due to interfacial condensation along the rectangular channel will be investigated. CFX Command Language (CCL) of ANSYS package was employed for simulation of these experiments with consideration of two-fluid model. Constant velocity inlet boundary condition according to superficial velocity of each phases is defined for gas and liquid phase separately, and constant pressure value is considered at the whole outlet. Surface turbulence model was implemented for both phases with source function of TKE and TEF near the free surface by calculation of interfacial area density value. All simulations were performed in transient scheme with time step of 0.0001 s–0.001 s. Also, the interfacial friction empirical correlation of stratified flow proposed by Kim et al. (1985) is used for drag coefficient at the interface.

4.1. Air/water stratified flow

Fabre et al. (1987) experiment of air and water stratified flow is selected to investigate variations of turbulence characteristics near the free surface. In the test section of this experiment, an adiabatic co-current air and water flow passes through a 12 m long, 20 cm wide and 10 cm high rectangular channel (Fig. 3). Air and water are separated at the channel inlet by a Plexiglas sheet that can be changed in different condition. To investigate different flow pattern of stratified flow, two different experiments, namely case 250 and case 400, will be simulated. The flow characteristics of each case are listed in Table 1. The inlet gas superficial velocity of case 250 is weak enough for waves to be negligible and the velocity of case 400 is high enough for waves circulation (Coste et al., 2012). The measurement of velocity and turbulence characteristic is performed at vertical line at a distance of 9.1 m from inlet. In this distance, the interfacial vertical velocity of water is about 0.0038 m/s for Case 250 and 0.0260 m/s for Case 400 demonstrating free surface motion in wavy flow regime. For selection of favorable grid size, three different meshes based on length (z), height(y) and width (x) variation are compared to investigate the effects of mesh size on water and air velocity profile. Fig. 4 depicts the results of this investigation for Case 250 versus normalized height calculated by consideration of mean water depth ($\bar{h}$) as follows:

$$h^*_{water} = \frac{y}{\bar{h}}$$
$$h^*_{air} = \frac{y - \bar{h}}{H_{channel} - \bar{h}} \tag{21}$$

The difference between coarsest mesh and the other, especially for air velocity, demonstrates unacceptably of the grid size. For evaluation of discretization error, Richardson extrapolation comparing the results of different grid sizes is used (Richardson and J Arthur Gaunt, 1927). Based on this method, Grid Convergence Index (GCI) demonstrating how much the solution approaches the asymptotic value is calculated as follows (Roache, 1997):

$$GCI_{i,i-1} = \frac{5}{4} \cdot \frac{\left|\frac{u_i - u_{i-1}}{u_{i-1}}\right|}{r^p - 1}. \tag{22}$$

Where "i" refers to grid size index, "r" is the grid refinement ratio and "p" is the order of computational method.

The acceptance value of GCI depends on problem and simulation methods, and would be assumed as discretization error. Usually, the value between 1 and 5% is considered for acceptance value of GCI (Ali et al., 2009; Roache, 1997). In addition to GCI, average relative error with consideration of experimental data is calculated to find the convergence of grid study procedure. The average values of GCI and relative error for air and water velocity of Case 250 are listed in Table 2.

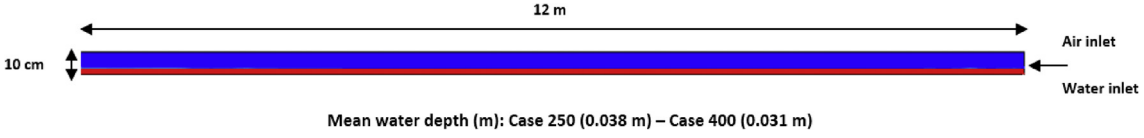

Fig. 3. Air/water cocurrent flow of Fabre et al. (1987) experiment in rectangular channel.

Table 1
Inlet boundary conditions for different scenario of Fabre et al. (1987) experiment.

	Case 250	Case 400
Water flow rate (m^3/s)	0.003	0.003
Air flow rate (m^3/s)	0.0454	0.0754
Bulk velocity of water (m/s)	0.395	0.476
Bulk velocity of air (m/s)	3.66	5.5
Mean water depth (m)	0.0380	0.0315

Table 2
Results of grid convergence study of Fabre's experiment.

	Mesh index	Mesh size (x,y,z)	Average Relative Error (%)	Average $GCI_{i,i-1}$ (%)
Water	1	(5 mm, 5 mm, 10 mm)	16.20	–
	2	(4 mm, 3 mm, 5 mm)	6.12	3.74
	3	(3 mm, 2.5 mm, 5 mm)	5.78	1.02
Air	1	(5 mm, 5 mm, 10 mm)	34.31	–
	2	(4 mm, 3 mm, 5 mm)	17.25	6.97
	3	(3 mm, 2.5 mm, 5 mm)	15.24	1.44

For water velocity, both $GCI_{3,2}$ and $GCI_{2,1}$ are less than 5% and average relative error shows minor difference between medium and finest mesh. Similar results are obtained for average relative error of air velocity between mentioned meshes. Also, the value of average $GCI_{3,2}$ shows the convergence of grid study procedure. So, the finest mesh in Table 2 is selected for CFD simulations.

Fig. 5 shows the velocity profile for water and air. For water section, the predicted profiles based on each model, except k-ω and k-ε without any modification, are in good agreement with experimental data near the wall and middle of water region. For mentioned regions, the result of k-ω with damping function turbulence model has a smaller deviation than the other. At the interface, a considerable overestimation of water velocity occurs for AIAD model while the other approaches have a small difference with experimental data. In air section, the velocity profile and maximum value location implies a same boundary condition at the interface and near upper wall. Although the result of k-ω with damping function model has a small deviation at the middle and upper part of air section, the interfacial air velocity shows a large difference between k-ω and experimental data. Due to same mass flow rate of each model, this discrepancy leads to moving upward of maximum value location and underestimation of interfacial velocity. The reason of this discrepancy, occurring for the other models, would be explained by turbulence effect in momentum equation. The vertical component of velocity would be neglected in smooth stratified flow regime at the interface. Also, the gradient of flow characteristics along flow direction are equal to zero in fully developed region. The consideration of these conditions simplifies the momentum equation without convection and pressure gradient terms. As a result, interphase momentum transfer (M_k in Eq. (2), including Drag force) and diffusion term play a signification role for evaluation of velocity profile. As the interfacial drag force is a function of air and water velocity difference, the following equation would be considered at the interface:

$$M_k = C_{drag,LG}|U_G - U_L| \approx -\nabla.\,[\alpha_k(\tau_k + \tau_k^T)] \tag{23}$$

Based on Boussinesq's hypothesis, the turbulence shear stress is calculated by velocity gradient and turbulence eddy viscosity. Fig. 6 depicts turbulence shear stress of k-ω with damping function model compared with experimental data. For water, turbulence stress and its gradient have a good agreement with experimental data leading to accurate prediction of water velocity. on the other hand, an overestimation of air turbulence stress occurs at the interface. Due to correct prediction of wall turbulence stress, this overestimation leads to reduction of turbulence stress gradient at the interface. Consequently, the predicted value of air velocity will decrease according to Eq. (23). As eddy viscosity is a function of TKE and TEF (Argyropoulos and Markatos, 2015), the evaluation of turbulence characteristics at the interface would demonstrate the shortcomings of proposed models.

Fig. 7 depicts TKE profile predicted by traditional eddy viscosity turbulence models. The overestimation of turbulence near the free surface is very clear in this figure as main shortcoming of k-ω and k-ε model for two-phase stratified flow. If only turbulence damping function is added to transport equation, the sharp increase of TKE will be captured as shown in Fig. 8. Also, the results of NEPTUNE CFD (Coste et al., 2008a) code and AIAD model (Höhne and Mehlhoop, 2014) are depicted in this figure. The same results for k-ω with damping function and NEPTUNE CFD code, capturing the overestimation of TKE, demonstrates the same effect of implementation of damping function and LIM for smooth stratified flow. Although implementation of damping function delivers better results for TKE, but the underestimation of turbulence near the free surface is noticeable, especially for air, and the simulation results have a significant difference with experimental data. By consideration of air TKE increasing at the interface, this difference implies that the implementation of turbulence damping function would lead to underestimation of turbulence for high value of TKE in smooth stratified flow (like Case 250). The underestimation of interfacial air TKE would be introduced as main reason of considerable air velocity deviation due to unacceptable boundary condition. In this condition, the TKE source function based on Eq. (20) dominates the turbulence profile and improve the prediction of air TKE at the interface. Although

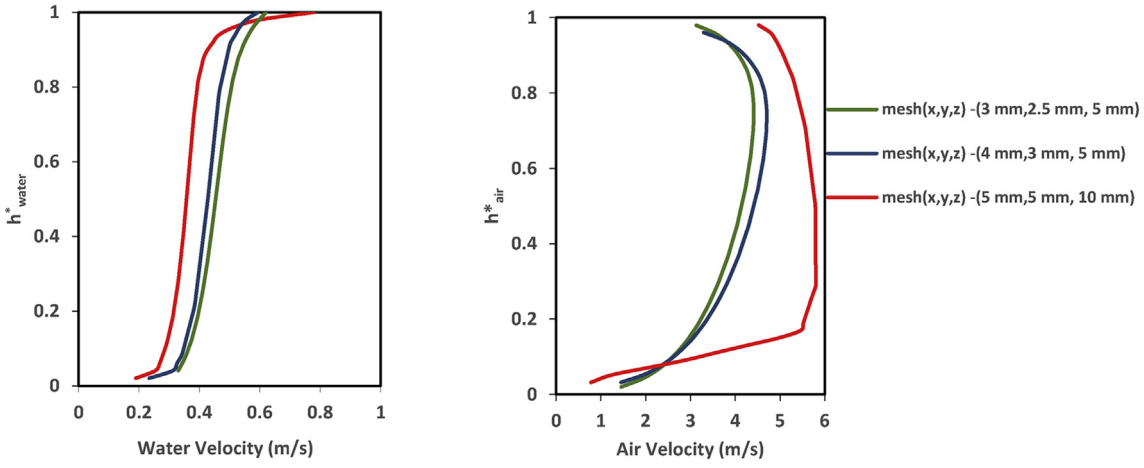

Fig. 4. Comparison between different meshes for prediction of water (left) and air (right) velocity in Case 250.

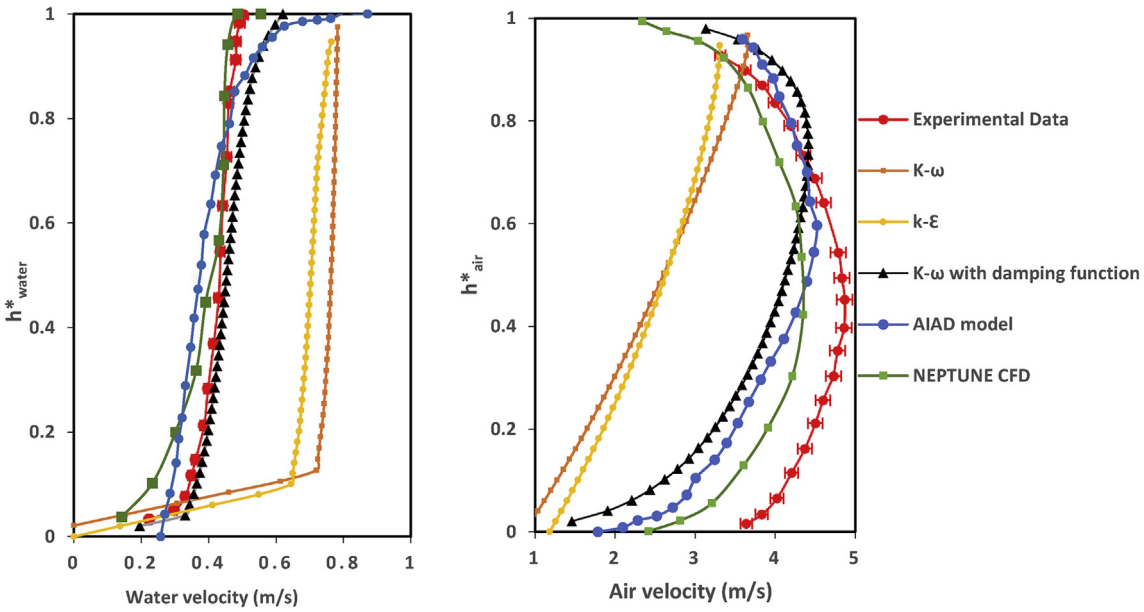

Fig. 5. Velocity profile of water (left) and air (right) of Case 250 with different turbulence model.

the underestimation of air interfacial TKE has minor effect on TKE profile far from the interface, the reduction of turbulence would occur in all regions when the flow regime changes to unstable and wavy stratified flow (like Case 400).

The next two-phase scenario of Fabre et al. (1987) experiment is based on increasing of air velocity to propagate fluctuation at the interface. In case 400, the flow rate of gas increases with no change of water flow rate. As a result, the depth of water film in channel reduces to 3.15 cm and minor change in water velocity. Fig. 9 shows the velocity profile of water and air. In comparison to case 250, the experimental data of water profile is same with minor differences. On the other hand, the shape of air velocity changes and maximum velocity moves to upper wall of channel. This condition implies that the boundary conditions of interface and wall are different and same treatment of interface and solid boundary would cause the other profile. To investigate the effect of selected boundary condition of Eq. (19), three different distances ($y^+ = 200$, $y^+ = 300$ and $y^+ = 400$) are considered as known boundary condition of this equation. If $y^+ = 200$ is selected as boundary condition near the interface, using TKE source do not give a significant advantage. But when this distance increases, the velocity at the interface have good agreement with experimental data and exhibit the effect of turbulence source in this region. Also, Fig. 10 depicts TKE profile for different models. As a result, simulation without TKE source leads to major underestimation of turbulence near the free surface. When TKE source is added to the simulation, this shortcoming of k-ω model will be improved. Therefore, for wavy flow (Case 400 of (Fabre et al. (1987)) experiment), application of damping function does not produce a good results especially in turbulence characteristics and the new source function of TKE would be useful for wavy flow.

4.2. Condensation in steam/water smooth stratified flow

The next test section reporting condensation rate and temperature gradient is known as LAOKOON test facility in Technical University of Munich (Goldbrunner et al., 2002). In this facility, subcooled water and steam are separately entered into a rectangular channel (about 1 m long and 0.128 m height) with adiabatic walls, which in the considered scenario has a pressure of about 6.97 bar (Fig. 11). The inlet steam is completely dry with temperature corresponding to the saturation temperature at the mentioned pressure. Therefore, the steam would be considered as isotherm fluid. In addition to overall condensation

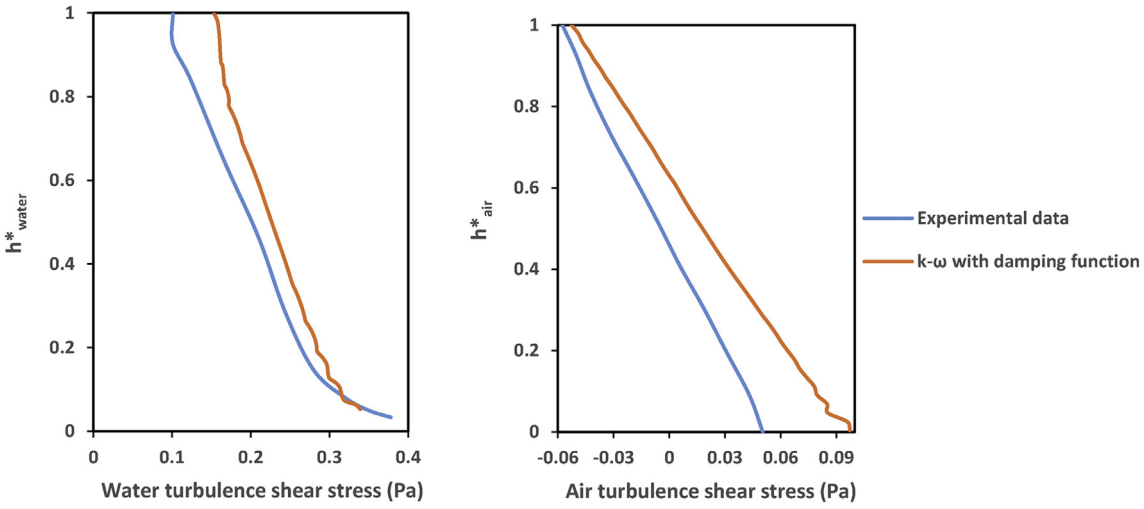

Fig. 6. Comparison of turbulence shear stress for water (left) and air (right) of Case 250.

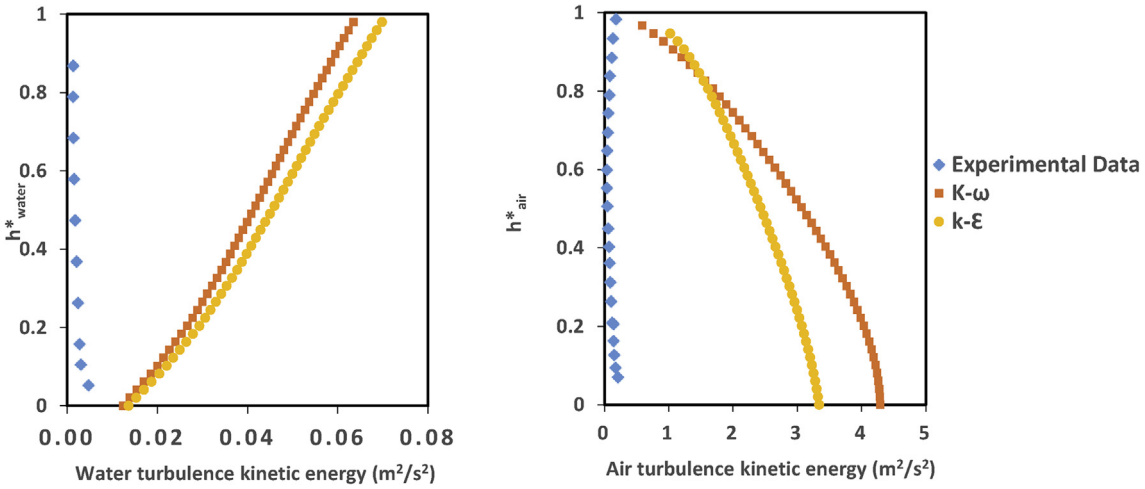

Fig. 7. Turbulence kinetic energy profile of water (left) and air (right) of Case 250 with k-ε and k-ω model.

reported about 40%, the water temperature is measured by 26 thermocouples at a distance of 79 cm from the inlet in vertical direction. According to the experimental evidence, this flow would be considered stationary and two-dimensional (Egorov et al., 2004; Goldbrunner et al., 2002). The boundary and initial conditions of the test section are listed in Table 3.

Two-dimension simulation is performed based on three different meshes condensed near the free surface and wall boundary to capture the effect of sub-layers. The results of average GCI and relative error are shown in Table 4. The convergence of relative error and the value less than 5% of $GCI_{3,2}$ imply that the finest mesh is appropriate for CFD simulations.

The interfacial HTC was calculated based on Eq. (4) and (5). Fig. 12 depicts the temperature profile along the measurement line compared with experimental data and Neptune _CFD simulation results (Galassi et al., 2008). The accuracy of temperature measurement is shown by horizontal error bars. In this figure the interfacial HTC was computed based on Shen et al. (2000) model. The result of overall condensation shows a considerable underestimation when only damping function is added at the interface for two meshes. Also, comparison of temperature profile with experimental data reveals two thermal separated layer with constant temperature due to underestimation of HTC at the interface. The results improve when the other source function of TKE is added to turbulence transport equation based on the proposed model in the current paper. In this condition, overall condensation increased and heat transfer occurs by eddy motion at the interface. Also, the results of simulation imply that the definition of constant C_1 in Eq. (16) would change the condensation rate and temperature gradient near the free surface. The difference between two proposed distances ($y^+ = 200$ and $y^+ = 400$) is about 7% for evaluation of condensation rate. The results of the other model according to Hughes and Duffey (1991) model are depicted in Fig. 13. Similar to previous results, without any special treatment for TKE, the overall condensation rate is lower than the reported value by experimental date. Unlike the previous model, the increasing of node number in vertical direction leads to reduction of condensation. Also, when the source function of TKE is added to the turbulence model, the increase of condensation rate is greater than Shen et al. (2000). The difference between two TKE boundary conditions is about 7% that is similar to the other models.

4.3. Condensation in wavy steam-water flow

The last test section is stratified flow of water and steam in a rectangular channel with 160.1 cm length, 30.48 cm width, and 6.35 cm height with adiabatic walls (Lim et al., 1984) (Fig. 14). The outlet pressure of channel is atmosphere pressure. In order to achieve different flow pattern, water and steam flow with different flow rates have been investigated. This test, carried out in 8 cases, leads to the observation of smooth, transient, and wavy interface shape. In this section, case 3 and 8 were selected to examine the condensation along the length of the channel. Based on experimental and simulation results, the shape of the free surface for case 3 and 8 is transition between smooth –wavy and

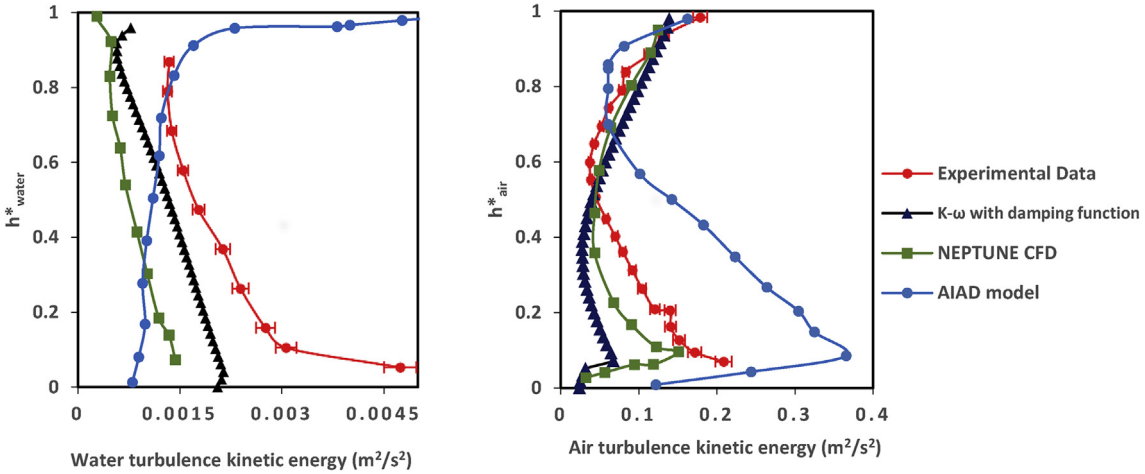

Fig. 8. Turbulence kinetic energy profile of water (left) and air (right) of Case 250 with turbulence damping function.

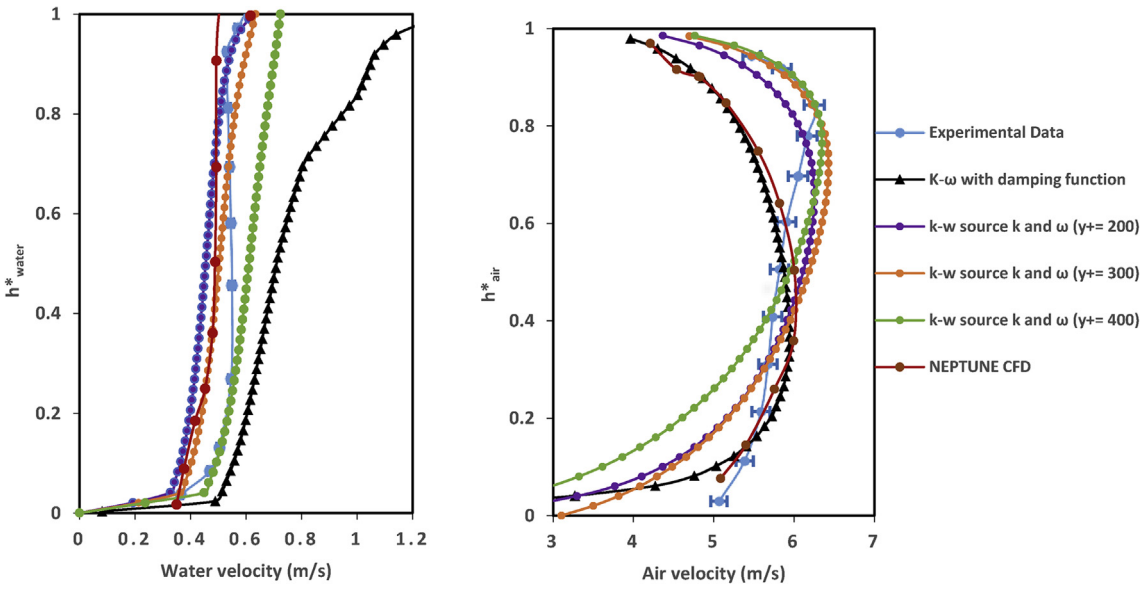

Fig. 9. Velocity profile of water (left) and air (right) of Case 400 with employment of different source functions.

wavy respectively (Kadi et al., 2015; Lim et al., 1984). The boundary conditions of two mentioned cases are listed in Table 5. Also, the boundary condition of TKE source was considered at two different distance from the interface ($y^+ = 200$ and $y^+ = 400$) to show the effect of the proposed assumption (Eq. (17)). To investigate grid size effect, two-dimension simulations were performed by employment of 25×100, 40×200 and 60×320 cells condensed near the interface and wall boundary to capture the effect of sub-layers. Similar to LAOKOON test section, Eq. (4) and (5) were considered as HTC at interface of steam and water. But, calculation of HTC based on Hughes and Duffey (1991) assumptions led to condensation of all steam before reaching the end of the channel and no improvement occurred when the TKE or TEF were added to the CFD code. Similar results of the mentioned model was reported by Yao et al. (2005). As a result, the following results are based on Shen et al. (2000) correlation for HTC.

The average value of relative error and GCI for the mentioned cells for case 3 and 8 are listed in Table 6. For each mesh, the source function of TKE ($y^+ = 400$) and TEF were employed at the interface. Based on average value of relative error and GCI, the finest grid is used for simulation of DCC. Fig. 15 and Fig. 16 show the reduction of steam mass flow along the channel length. In these figures, the accuracy of mass flow measurement, estimated by energy balance and mass flow comparison between inlet and measurement points, is depicted by vertical error bars. For both cases, the implementation of TEF source as damping function leads to underestimation of condensation rate. The mentioned shortcoming is the same for both grids and a minor reduction of condensation occurs when the grid numbers in channel height increase. According to Figs. 15 and 16, the employment of TKE source function increases HTC and condensation at the interface and improves the mass flow rate along the channel length. So, it can be concluded that the source function of TKE plays a significant effect on interfacial mass transfer. If zero boundary condition of TKE like wall is considered for calculation of turbulence characteristics at the interface, the condensation rate will be underestimated. Also, the change of the specified distance to define the boundary condition of the Eq. (14) ($y^+ = 200$ and $y^+ = 400$), has a minor reduction of condensation rate due to increasing of TKE at the interface.

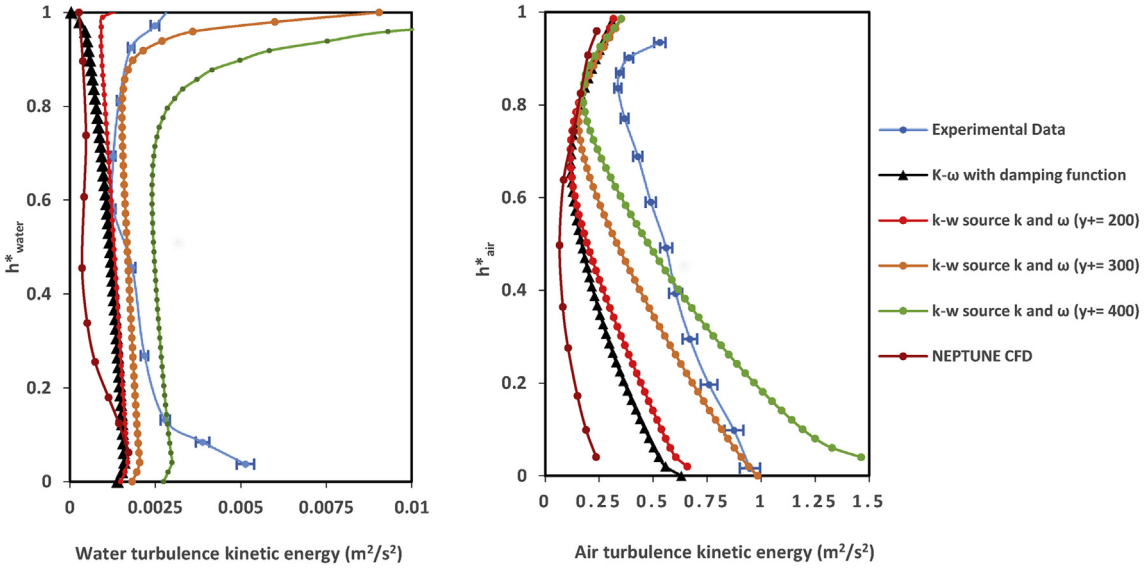

Fig. 10. Turbulence kinetic energy profile of water (left) and air (right) of Case 400 with employment of different source functions.

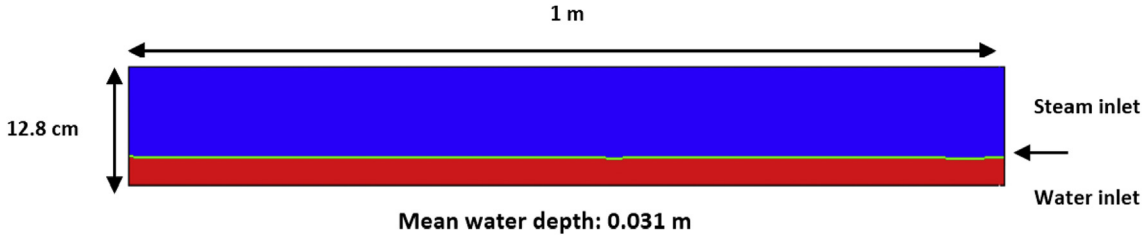

Fig. 11. Steam/water cocurrent flow in LAOKOON test facility.

Table 3
Inlet boundary conditions for LAOKOON test facility.

Water inlet velocity (m/s)	0.28
steam inlet velocity (m/s)	3.2
Water inlet temperature (°C)	27
Steam inlet temperature (°C)	164.7
Mean water depth (m)	0.031
Pressure (bar)	6.97

Table 4
Results of grid convergence procedure in LAOKOON test facility.

Mesh index	Number of elements (n_y,n_z)	Average Relative Error (%)	Average $GCI_{i,i-1}$ (%)
1	(30,60)	31.20	–
2	(40,100)	11.46	8.52
3	(70,200)	9.45	0.97

5. Conclusion

Simulation of steam/water stratified flow plays a significant role for thermal-hydraulic analysis of two-phase PTS in PWRs. In the cold leg of PWR, condensation of seam and interfacial mass transfer as complex 3D phenomena needs a special attention for CFD simulation after LOCA. As HTC is calculated based on turbulence length and velocity scale, the exact turbulence model should be implemented to capture all requirements of mass and energy balance. The high gradient of some flow characteristics like velocity and TKE dictates some especial limitations for application of common two-equation eddy viscosity models. The overestimation of TKE due to high gradient of velocity is one of these limitations affecting the value of HTC. This overestimation which also occurs near solid boundary condition would be solved by employment of turbulence damping function at the interface. The application of this function significantly decreases TKE and leads to special boundary condition at the steam/water interface. The evaluation of experimental results and reduced equations reveal that this boundary condition is different from real condition. Therefore, the other boundary condition of TKE was proposed based on the definition of TKE source function. Due to lack information about TKE profile at the interface, some reasonable assumptions based on TKE in the bulk of water and steam were considered for definition of proposed function.

The variations of HTC, temperature gradient and condensation rate were investigated to assess the effect of new turbulence source function at the interface. The first step for this goal was performed by simulation of air/water isothermal flow of Fabre et al. (1987) experiment. In this experiment, velocity and TKE in both phases have been measured for smooth and wavy stratified flow. The comparison of the simulation results with experimental data showed that implementation of damping function improves the velocity profile and overestimation of TKE at the interface. But, when the velocity of gas phase increases and flow pattern shift to transient region, a considerable underestimation of TKE occurs due to zero boundary condition of TKE. This shortcoming improves by employment of proposed TKE source function. By consideration of the modification of TKE in isothermal stratified flow, steam/water flow in Lim et al. (1984) and LAOKOON (Goldbrunner et al., 2002) test sections was simulated to assess the improvement of thermal characteristics. In these experiments, HTC was calculated based on Hughes and Duffey (1991) and Shen et al. (2000) models. For both models, implementation of damping function leads to high temperature gradient at the interface and underestimation of condensation rate. As the turbulence velocity scale has a direct relation with TKE, it can be concluded that underestimation of TKE increases the eddy contact time at the interface. If the

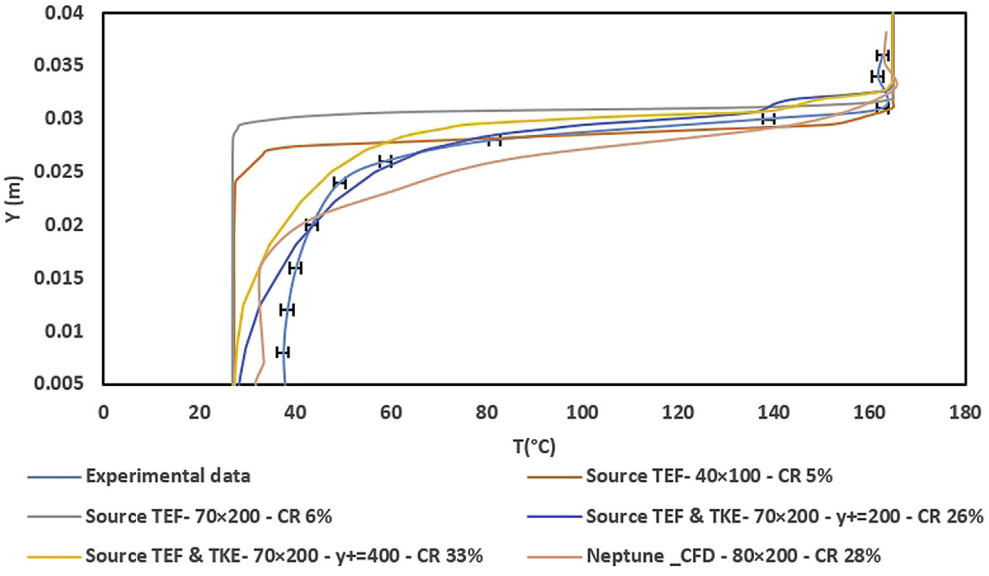

Fig. 12. Temperature profile in vertical direction at the distance of 79 cm from the inlet with Shen et al. (2000) model; (CR: Condensation Rate).

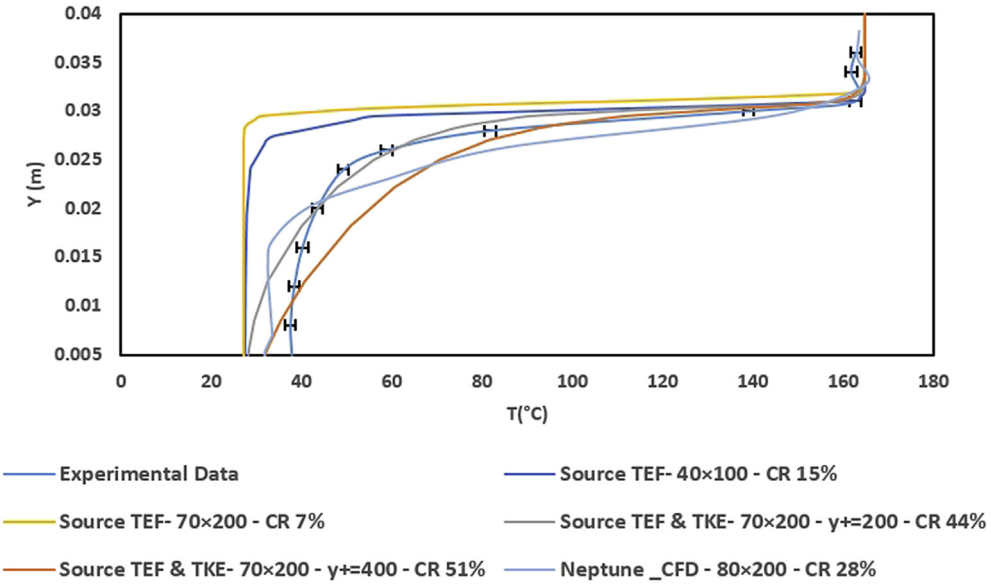

Fig. 13. Temperature profile at the distance of 79 cm from the inlet with Hughes and Duffey (1991) model; (CR: Condensation Rate).

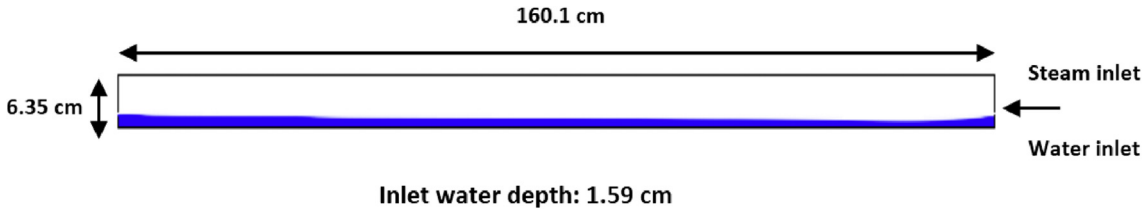

Fig. 14. Steam/water cocurrent flow of (Lim et al., 1984) experiment in a rectangular channel.

Table 5
Boundary conditions for Lim et al. (1984) experiment.

	Case 3	Case 8
Water mass flow rate (kg/s)	0.657	1.44
Steam mass flow rate (kg/s)	0.089	0.126
Water inlet temperature (°C)	25	25
Steam inlet temperature (°C)	121	125
Inlet water depth (m)	0.0159	0.0159

Table 6
Results of grid convergence study in case 3 and 8 of Lim et al. (1984) experiment.

	Mesh index	Number of elements (n_y,n_z)	Average Relative Error (%)	Average $GCI_{i,i-1}$ (%)
Case 3	1	(25, 100)	28.51	–
	2	(40, 200)	14.11	7.58
	3	(60, 320)	12.66	0.82
Case 8	1	(25, 100)	25.67	–
	2	(40, 200)	9.88	6.91
	3	(60, 320)	8.37	0.75

TKE source function is added to transport equations, the predicted temperature profile in water and overall condensation will in a better agreement with experimental data. For Hughes and Duffey (1991) model, the difference between implementation of TKE source and damping function is more that these results of Shen et al. (2000) model. As a result, the variations of turbulence characteristics have more impact on HTC base on Hughes and Duffey (1991) model. Similar improvements of condensation along the horizontal channel of Lim experiment were observed for (Shen et al. (2000)) model. On the other hand, calculation of HTC based on Hughes and Duffey (1991) model leads to condensation of the total inlet steam based on two mentioned source function of TEF and TKE.

Calculation of HTC based on turbulence length and velocity scale and different approaches for turbulence modeling reveals the modeling problems as current research area of CFD methods. According to the simulation results of this paper, the modification of turbulence boundary conditions at the interface of two-phase stratified flow significantly changes HTC and temperature gradient based on SRT. These changes have more impacts on HTC of (Hughes and Duffey (1991)) model and in some experiments, no improvement of condensation would occur even with TKE and TEF source functions. As a consequence, the energy transfers from large eddies to small eddies based on Kolmogorov theory needs the other assumptions at gas entrainment would affect turbulence boundary conditions and source functions at the interface. For consideration of these effects, the experimental data of turbulence characteristics is needed for different flow inlet boundary condition and interface shape to evaluate turbulence production of each phenomenon.

In addition to experimental data development, improvement of interfacial turbulence modeling and its effect on condensation rate should be considered as the other research area. Although the proposed turbulence model can improve the shortcoming of traditional model in a simple channel, different geometry scales and flow characteristics would impose some limitations on the turbulence source function implementation. Consequently, the definition of this function would be done by consideration of related nondimensional number. Also, application of two-fluid model dictates some limitations for simulation of gas and liquid dispersed flow at the interface. This new phases would change the heat transfer coefficient, turbulence energy and interface shape. Also, calculation of HTC based on SRT has no dependency on flow regime affecting the mentioned parameters. So, the other

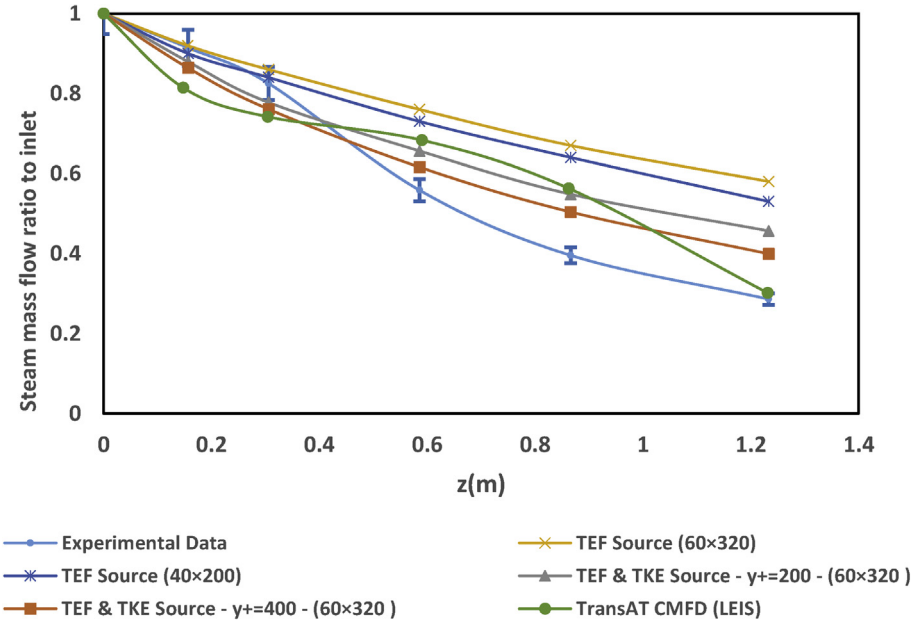

Fig. 15. Mass flow reduction of steam along the channel length in case 3 of Lim et al. (1984).

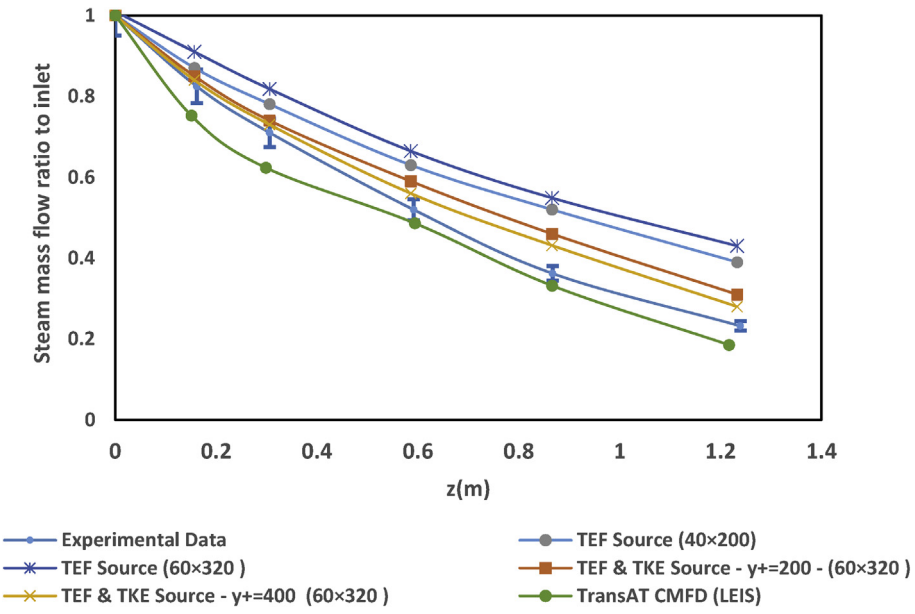

Fig. 16. Mass flow reduction of steam along the channel length in case 8 of Lim et al. (1984).

computational study should be done to survey the effects of flow regime on turbulence length and velocity scale used for HTC evaluation.

References

Akira, M., Fiji, H., Takamoto, S., 1992. Prediction of heat transfer by direct contact condensation at a steam-subcooled water interface. Int. J. Heat Mass Tran. 35, 101–109.

Ali, M.S.M., Doolan, C.J., Wheatley, V., 2009. Grid convergence study for a two-dimensional simulation of flow around a square cylinder at a low Reynolds number. In: Witt & MP Schwarz, P.J. (Ed.), Seventh International Conference on CFD in the Minerals and Process Industries, pp. 1–6.

Apanasevich, P., Lucas, D., Beyer, M., Szalinski, L., 2015. CFD based approach for modeling direct contact condensation heat transfer in two-phase turbulent stratified flows. Int. J. Therm. Sci. 95, 123–135.

Ayati, A., Kolaas, J., Jensen, A., Johnson, G., 2016. The effect of interfacial waves on the turbulence structure of stratified air/water pipe flow. Int. J. Multiphas. Flow 78, 104–116.

Ayati, A.A., Kolaas, J., Jensen, A., Johnson, G.W., 2014. A PIV investigation of stratified gas–liquid flow in a horizontal pipe. Int. J. Multiphas. Flow 61, 129–143.

Banerjee, S., 1990. Turbulence structure and transport mechanisms at interfaces. In: Ninth International Heat Transfer Conference, pp. 3957418.

Banerjee, S., Lakehal, D., Fulgosi, M., 2004. Surface divergence models for scalar exchange between turbulent streams. Int. J. Multiphas. Flow 30, 963–977.

Bestion, D., 2010. Extension of CFD codes application to two-phase flow safety problems. Nucl. Eng. Technol. 42, 365–376.

Bian, H., Sun, Z., Ding, M., Zhang, N., 2017. Local phenomena analysis of steam condensation in the presence of air. Prog. Nucl. Energy 101, 188–198.

Brocchini, M., Peregrine, D., 2001. The dynamics of strong turbulence at free surfaces. Part 1. Description. J. Fluid Mech. 449, 225–254.

Argyropoulos, C.D., Markatos, N.C., 2015. Recent advances on the numerical modelling of turbulent flows. Appl. Math. Model. 39 (2), 693–732.

Ceuca, S.C., Macián-Juan, R., 2012. CFD simulation of direct contact condensation with ANSYS CFX using locally defined heat transfer coefficients. In: 2012 20th International Conference on Nuclear Engineering and the ASME 2012 Power Conference. American Society of Mechanical Engineers, pp. 429–437.

Collier, J.G., Thome, J.R., 1994. Convective Boiling and Condensation. Clarendon Press.

Coste, P., Laviéville, J., Pouvreau, J., Baudry, C., Guingo, M., Douce, A., 2012. Validation of the large interface method of NEPTUNE_CFD 1.0. 8 for pressurized thermal shock (PTS) applications. Nucl. Eng. Des. 253, 296–310.

Coste, P., Pouvreau, J., Laviéville, J., Boucker, M., 2008a. Status of a Two-phase CFD

Approach to the PTS Issue.
Coste, P., Pouvreau, J., Laviéville, J., Boucker, M., 2008b. A two-phase CFD approach to the PTS problem evaluated on COSI experiment. In: 16th International Conference on Nuclear Engineering. American Society of Mechanical Engineers, pp. 573–581.
Danckwerts, P., 1951. Significance of liquid-film coefficients in gas absorption. Ind. Eng. Chem. 43, 1460–1467.
Egorov, Y., Boucker, M., Martin, A., Pigny, S., Scheuerer, M., Willemsen, S., 2004. Validation of CFD codes with PTS-relevant test cases. In: 5th Euratom Framework Programme ECORA Project.
Fabre, J., Masbernat, L., Suzanne, C., 1987. Experimental data set no. 7: stratified flow, part I: local structure. Multiphas. Sci. Technol. 3.
Gada, V.H., Tandon, M.P., Elias, J., Splawski, A., Lo, S., 2016. Simulation of direct contact condensation using large scale interface multifluid model. In: 2016 24th International Conference on Nuclear Engineering. American Society of Mechanical Engineers, V004T010A023–V004T010A023.
Galassi, M.C., Coste, P., Morel, C., Moretti, F., 2008. Two-phase flow simulations for PTS investigation by means of Neptune_CFD code. Sci. Technol. Nucl. Install. 2009.
Goldbrunner, M., Karl, J., Hein, D., 2002. Experimental Investigation of Heat Transfer Phenomena during Direct Contact Condensation in the Presence of Non Condensable Gas by Means of the Linear Raman Spectroscopy, Laser Techniques for Fluid Mechanics. Springer, pp. 113–131.
Griffiths, M.J., Schlegel, J.P., Hibiki, T., Ishii, M., Kinoshita, I., Yoshida, Y., 2014. Phenomena identification and ranking table for thermal-hydraulic phenomena during a small-break LOCA with loss of high pressure injection. Prog. Nucl. Energy 73, 51–63.
Higbie, R., 1935. The Rate of Absorption of a Pure Gas into Still Liquid during Short Periods of Exposure.
Höhne, T., Lucas, D., 2011. Numerical simulations of counter-current two-phase flow experiments in a PWR hot leg model using an interfacial area density model. Int. J. Heat Fluid Flow 32, 1047–1056.
Höhne, T., Mehlhoop, J.-P., 2014. Validation of closure models for interfacial drag and turbulence in numerical simulations of horizontal stratified gas–liquid flows. Int. J. Multiphas. Flow 62, 1–16.
Hughes, E., Duffey, R., 1991. Direct contact condensation and momentum transfer in turbulent separated flows. Int. J. Multiphas. Flow 17, 599–619.
Hunt, J., Graham, J., 1978. Free-stream turbulence near plane boundaries. J. Fluid Mech. 84, 209–235.
IAEA, 2003. Guidelines on pressurized thermal shock analysis for WWER nuclear power plants.
Ishii, M., Hibiki, T., 2010. Thermo-fluid Dynamics of Two-phase Flow. Springer Science & Business Media.
Kadi, R., Aissani, S., Bouam, A., 2015. Numerical simulation of the direct contact condensation phenomena for PTS-related in single and combined-effect thermal hydraulic test facilities using TransAT CMFD code. Nucl. Eng. Des. 293, 346–356.
Kalitzin, G., Medic, G., Iaccarino, G., Durbin, P., 2005. Near-wall behavior of RANS turbulence models and implications for wall functions. J. Comput. Phys. 204, 265–291.
Kim, H., Lee, S., Bankoff, S., 1985. Heat transfer and interfacial drag in countercurrent steam-water stratified flow. Int. J. Multiphas. Flow 11, 593–606.
Kolmogorov, A.N., 1941. Dissipation of Energy in Locally Isotropic Turbulence. Dokl. Akad. Nauk SSSR. JSTOR, pp. 16–18.
Lakehal, D., 2010. LEIS for the prediction of turbulent multifluid flows applied to thermal-hydraulics applications. Nucl. Eng. Des. 240, 2096–2106.
Lakehal, D., Labois, M., 2011. A New modelling strategy for phase-change heat transfer in turbulent interfacial two-phase flow. Int. J. Multiphas. Flow 37, 627–639.
Lamb, H., 1932. Hydrodynamics. Cambridge university press.
Li, S.Q., Wang, P., Lu, T., 2015. Numerical simulation of direct contact condensation of subsonic steam injected in a water pool using VOF method and LES turbulence model. Prog. Nucl. Energy 78, 201–215.
Lim, I., Tankin, R., Yuen, M., 1984. Condensation measurement of horizontal cocurrent steam/water flow. J. Heat Tran. 106, 425–432.
Lin, P., Hanratty, T., 1986. Prediction of the initiation of slugs with linear stability theory. Int. J. Multiphas. Flow 12, 79–98.
Liovic, P., Lakehal, D., 2007. Interface–turbulence interactions in large-scale bubbling processes. Int. J. Heat Fluid Flow 28, 127–144.
Lips, S., Meyer, J.P., 2012. Experimental study of convective condensation in an inclined smooth tube. Part I: inclination effect on flow pattern and heat transfer coefficient. Int. J. Heat Mass Tran. 55, 395–404.
Lucas, D., Bestion, D., Bodèle, E., Scheuerer, M., F D'Auria, D.M., Smith, B., Tiselj, I., Martin, A., Lakehal, D., Seynhaeve, J., 2007. On the simulation of two-phase flow pressurized thermal shock (PTS). In: 12th International Topical Meeting on Nuclear Reactor Thermal Hydraulics (NURETH-12).
Milne-Thompson, L.M., 1968. Theoretical Hydrodynamics, fifth ed. MacMillan, London, pp. 1.
Nourgaliev, R.R., Liou, M.-S., Theofanous, T.G., 2008. Numerical prediction of interfacial instabilities: sharp interface method (SIM). J. Comput. Phys. 227, 3940–3970.
Reboux, S., Sagaut, P., Lakehal, D., 2006. Large-eddy simulation of sheared interfacial flow. Phys. Fluids 18, 105105 (1994-present).
Ren, W.Y., Fu, X.L., Tian, W.X., Dong, B., Bian, J.W., Yu, G.J., Yang, Y.H., Qiu, S.Z., Su, G.H., 2016. ECC condensation research in T-junction. Prog. Nucl. Energy 92, 62–70.
Richardson, L.F., J Arthur Gaunt, B., 1927. VIII. The deferred approach to the limit. Phil. Trans. Roy. Soc. Lond. 226, 299–361.
Roache, P.J., 1997. Quantification of uncertainty in computational fluid dynamics. Annu. Rev. Fluid Mech. 29, 123–160.
Roman, A.J., Kreitzer, P.J., Ervin, J.S., Hanchak, M.S., Byrd, L.W., 2016. Flow pattern identification of horizontal two-phase refrigerant flow using neural networks. Int. Commun. Heat Mass Tran. 71, 254–264.
Shen, L., Triantafyllou, G.S., Yue, D.K., 2000. Turbulent diffusion near a free surface. J. Fluid Mech. 407, 145–166.
Štrubelj, L., Ézsöl, G., Tiselj, I., 2010. Direct contact condensation induced transition from stratified to slug flow. Nucl. Eng. Des. 240, 266–274.
Thorpe, S., 1969. Experiments on the instability of stratified shear flows: immiscible fluids. J. Fluid Mech. 39, 25–48.
Vallée, C., Höhne, T., Prasser, H.-M., Sühnel, T., 2008. Experimental investigation and CFD simulation of horizontal stratified two-phase flow phenomena. Nucl. Eng. Des. 238, 637–646.
Versteeg, H.K., Malalasekera, W., 2007. An Introduction to Computational Fluid Dynamics: the Finite Volume Method. Pearson Education.
Wilcox, D.C., 1998. Turbulence Modeling for CFD. DCW industries, La Canada, CA.
Yao, W., Bestion, D., Coste, P., Boucker, M., 2005. A three-dimensional two-fluid modeling of stratified flow with condensation for pressurized thermal shock investigations. Nucl. Technol. 152, 129–142.